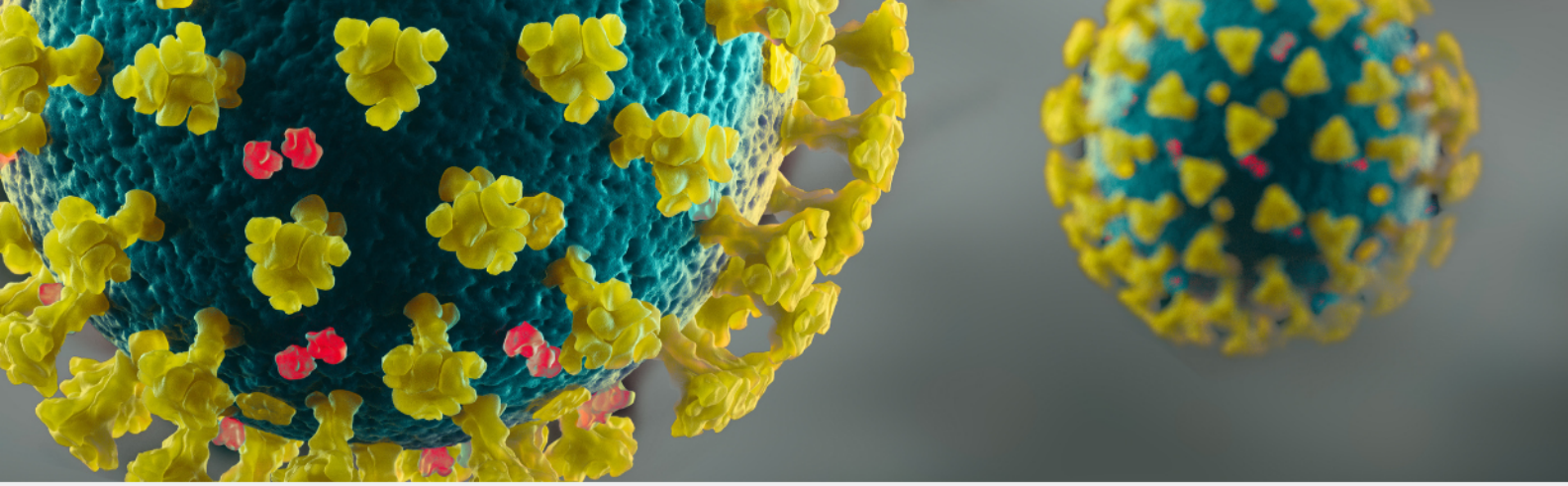

Vaccine Discovery and Development: Lessons from COVID-19

Free eBook

Emerging infectious diseases (EIDs) can evolve into a global healthcare crisis or pandemic. Scientists have previously required years to develop vaccines or therapeutics. The use of high throughput technology can greatly broaden the insights collected during discovery, augment efficiency and safety of handling EIDs, and shorten timelines.

Download this publication for an overview of many lessons learned in virology, immunology, and vaccine research during COVID-19 vaccine development.

Download here

SARTORIUS

CURRENT PROTOCOLS
A Wiley Brand

THE FASEB JOURNAL • RESEARCH • www.fasebj.org

The histone demethylase KDM5A is required for the repression of astrocytogenesis and regulated by the translational machinery in neural progenitor cells

Sun-Young Kong, Woosuk Kim, Ha-Rim Lee, and Hyun-Jung Kim[1]
Laboratory of Molecular and Stem Cell Pharmacology, College of Pharmacy, Chung-Ang University, Seoul, South Korea

ABSTRACT: Histone demethylases are known to play important roles in the determination of the fate of stem cells and in cancer progression. In this study, we show that the lysine 4 of histone H3 (H3K4), lysine-specific demethylase 5A (KDM5A) is essential for the repression of astrocyte differentiation in neural progenitor cells (NPCs), and its expression is regulated by translational machinery. Knockdown of KDM5A in NPCs increased astrocytogenesis, and conversely, KDM5A overexpression reduced the transcriptional activity of the *Gfap* promoter. Induction of astrocytogenesis by ciliary neurotrophic factor (CNTF) or small interfering RNA-induced knockdown of KDM5A decreased KDM5A recruitment to the *Gfap* promoter and increased H3K4 methylation. The transcript level of *Kdm5a* was high, whereas KDM5A protein level was low in CNTF induced astrocytes. During astroglial differentiation, translational activity indicated by the phosphorylation of eukaryotic translation initiation factor (eIF)4E was decreased. Treatment of NPCs with the cercosporamide, a MAPK-interacting kinases inhibitor, reduced eIF4E phosphorylation and KDM5A protein expression, increased GFAP levels, and enhanced astrocytogenesis. These data suggest that KDM5A is a key regulator that maintains NPCs in an undifferentiated state by repressing astrocytogenesis and that its expression is translationally controlled during astrocyte differentiation. Thus, KDM5A is a promising target for the modulation of NPC fate.—Kong, S.-Y., Kim, W., Lee, H.-R., Kim, H.-J. The histone demethylase KDM5A is required for the repression of astrocytogenesis and regulated by the translational machinery in neural progenitor cells. FASEB J. 32, 1108–1119 (2018). www.fasebj.org

KEY WORDS: epigenetics · H3K4 demethylase · NSC differentiation · eIF-4E · MAPK-interacting kinase

Neural stem cells (NSCs) have the ability to self-renew and to differentiate into multiple cell types including neurons, astrocytes, and oligodendrocytes (1). One of the methods of culturing these cells comprises the generation of undifferentiated floating spheres termed neurospheres; however, most of the cells in neurospheres generated from developing fetal brains show limited self-renewal and a reduced capacity to produce neurons at later passages. Thus, we have termed them neural progenitor cells (NPCs) (2, 3). NSCs and NPCs proliferate in the presence of growth factors and differentiate in the absence of mitogens.

The generation of specific cell types from NSCs or NPCs involves a variety of genes, each of which must be precisely expressed in a timely manner. Achieving this precise control of gene expression requires not only the genetic information embedded in DNA, but also the correct functioning of epigenetic regulation mechanisms, such as DNA methylation, histone modification, chromatin remodeling, and noncoding RNAs (4). We and others have reported on the important function of histone demethylases in the determination of cell fate (5–9). Histone demethylases are known to remove methyl moiety from histones and include the flavin-dependent amine oxidases, lysine-specific histone demethylase (LSD)1 and -2 (grouped as KDM1), whose substrates comprise mono- and dimethyl lysines, and the large Jumonji C (JmjC) domain-containing demethylase family (10). On the basis of homology, the JmjC domain-containing demethylase family consists of 30 members, 18 of which have been identified to exhibit histone demethylase activity, and is categorized into 6 subfamilies: KDM2–7. The JmjC domain-containing histone demethylases catalyze the removal of a methyl group from trimethylated, as well as mono- and dimethylated, lysine residues of histones.

ABBREVIATIONS: BTZ, bortezomib; Cerco, cercosporamide; ChIP, chromatin immunoprecipitation; CNTF, ciliary neurotrophic factor; EGF, epidermal growth factor; eIF, eukaryotic translation initiation factor; FGF, fibroblast growth factor; GFAP, glial fibrillary acidic protein; HA, hemagglutinin; H3K4, lysine 4 of histone 3; H34me, methylated lysine 4 of histone H3; HEK, human embryonic kidney cell; KDM5A, lysine-specific demethylase 5A; m7G, 7-methylguanosine; miRNA, microRNA; MNK, MAPK-interacting kinase; NICD, notch intracellular domain; NPC, neural progenitor cell; NSC, neural stem cell; siRNA, small interfering RNA; STAT, signal transducer and activator of transcription; TSS, transcription start site; TUBB, tubulin β

[1] Correspondence: Laboratory of Molecular and Stem Cell Pharmacology, College of Pharmacy, Chung-Ang University, 221 Heukseok-dong Dongjak-gu, Seoul 156-756, South Korea. E-mail: hyunjungkim@cau.ac.kr

doi: 10.1096/fj.201700780R
This article includes supplemental data. Please visit *http://www.fasebj.org* to obtain this information.

0892-6638/18/0032-1108 © FASEB

The lysine-specific demethylase 5 (KDM5) subfamily consists of KDM5A (JARID1A/RBP2), KDM5B (JARID1B/PLU1), KDM5C (JARID1C/SMCX), and KDM5D (JARID1D/SMCY) and is specific to di- and trimethylated lysine 4 of histone H3 (H3K4me2 and H3K4me3) (11). Recent evidence has shown that KDM5A has a critical function in cancer biology as an oncogene and emphasizes the clinical importance of the developing KDM5A-specific inhibitors as novel cancer treatments that may reduce cancer cell drug resistance (12–14). The tumor-suppressive effect of the retinoblastoma protein (pRB) is partially affected by its ability to sequester its binding partner, KDM5A (15). It is also reported that KDM5A is necessary for natural killer cell activation, by associating with p50 to suppress the suppressor of cytokine signaling 1 that inhibits the phosphorylation and nuclear localization of signal transducer and activator of transcription (STAT)4 (16). A genome-wide study recently identified various KDM5A target genes, including differentiation-independent genes that are essential for mitochondrial function and DNA/RNA metabolism (17). Other KDM5A targets were found to be differentiation dependent, including those critical for cell-cycle progression. The recently identified roles of KDM5A in cancer-cell proliferation and survival suggest that it may be critical to stem and progenitor cell proliferation; however, the roles of KDM5A during brain development and neural cell proliferation or specification or both have not been determined.

Translational control of specific mRNAs is also critical for gene expression and regulates a variety of cellular and developmental processes (18). The protein translation process comprises 3 steps: initiation, elongation, and termination. In most circumstances, the greatest degree of regulation occurs during the initiation step, when target mRNA is recruited to the ribosome (19). Transcribed mRNAs contain the 5′-7-methylguanosine (m7G) cap structure that provides binding sites for initiation factors, facilitates ribosome recruitment, and is therefore essential for translation. Specifically, translation initiation begins with the binding of the eukaryotic translation initiation factor (eIF)4F complex to the 5′-m7G cap (20). This eIF4F complex comprises eIF4A, eIF4G, and eIF4E (the cap-binding subunit) and its formation is dependent on eIF4E availability (19, 20). The MAPK-interacting kinases (MNKs) are activated by MAPK, and phosphorylate eIF4E at Ser209; however, the exact biologic role of this phosphorylation remains controversial (21). Recently published research has revealed that eIF4E dysregulation is associated with carcinogenesis, and the inhibition of protein translation (22). Nevertheless, the impact of translation on cell fate determination during brain development is not known yet.

In the present study, we demonstrated that KDM5A plays an important role in maintaining NPCs as multipotent cells by repressing astrocyte differentiation. The *Kdm5a* mRNA level was much higher in ciliary neurotrophic factor (CNTF)–induced differentiated astrocytes than in NPCs. With this study, we provide evidence that translational activity is down-regulated during astrocytogenesis and KDM5A expression is regulated by the translational machinery. These data suggest that KDM5A is a promising target molecule for NPC fate modulation.

MATERIALS AND METHODS

Cell culture

NPCs were cultured as previously described (23). Animal experiments were performed in strict accordance with the Chung-Ang University and the National Institutes of Health (Bethesda, MD, USA) *Guide for the Care and Use of Animals*. In brief, NPCs were isolated from the cortex of embryonic day (E) 14 Sprague-Dawley rats (Orient Bio, Seongnam, South Korea) and cultured in DMEM/F-12 Nutrient Mixture (DMEM/F12) supplemented with 1% (v/v) antibiotic-antimycotic, 2% (v/v) B27 (Thermo Fisher Scientific, Waltham, MA, USA), and 20 ng/ml epidermal growth factor (EGF) and fibroblast growth factor (FGF)-2 (Chemicon, Temecula, CA, USA). To maintain self-renewal and an undifferentiated state, NPCs were cultured in the presence of EGF and FGF2. For astrocytic differentiation, NPCs were treated with 10 ng/ml recombinant rat CNTF (Millipore-Sigma, Billerica, MA, USA) in the absence of growth factors. As indicated, cultures were supplemented with 0.1% DMSO, 5 μM cercosporamide (Cerco; Millipore-Sigma), 5 μM MG132, 25 nM bortezomib (BTZ) (Millipore-Sigma), and 50 μM U0126 (Cell Signaling Technology, Danvers, MA, USA).

Human embryonic kidney (HEK) 293T cells were cultured in DMEM/F12 containing 1% (v/v) antibiotic-antimycotic and 5% (v/v) fetal bovine serum (TaKaRa Bio, Mountain View, CA, USA).

Small interfering RNA nucleofection

Nucleofection was performed using the Amaxa 4D-Nucleofector System (Lonza, Basel, Switzerland). After 1 wk of neurosphere expansion, NPCs were dissociated and nucleofected with small interfering RNAs (siRNAs) targeting rat *Kdm5a*, *Kdm5b*, *Kdm5d*, or *Eif4e* mRNA (Supplemental Table S1), or with nontargeting siRNA (negative control siRNA; GenePharma, Shanghai, China). For each nucleofection, 5×10^6 cells were resuspended in 100 μl of P4 Primary Cell Solution (Lonza) containing 40 pmol siRNA, and pulsed with the DC104 program. After nucleofection, the cells were cultured in the presence of 40 ng/ml EGF and 20 ng/ml FGF2.

Real-time RT-PCR

Total RNA was extracted with Trizol reagent (Thermo Fisher Scientific). First-strand cDNA was synthesized from 1 μg of total RNA with a QuantiTect Reverse Transcription Kit (Qiagen, Limburg, The Netherlands). RT-PCR was performed using iQ SYBR Green supermix (Bio-Rad, Hercules, CA, USA), with the following cycling conditions: initial activation at 95°C for 3 min, followed by 40 cycles of denaturation at 95°C for 10 s, annealing at 58°C for 15 s, and extension at 72°C for 20 s. The cDNA primer sets are described in Supplemental Table S2; the housekeeping gene *Gapdh* was used as an internal control.

Luciferase reporter assay

HEK293T cells were cotransfected using Lipofectamine 2000 Reagent (Thermo Fisher Scientific), with 1750 ng of either pcDNA3-HA-KDM5A (kindly provided by Dr. Kaelin, Dana-Farber Cancer Institute and Brigham and Women's Hospital, Harvard Medical School, Boston, MA, USA) or empty-pcDNA3 vector, 375 ng of pGL3 firefly luciferase vector containing either

the glial fibrillary acidic protein (*Gfap*) promoter (pGfa2-luc3; kindly provided by Dr. Brenner through the Alabama Neuroscience Blueprint Core, University of Alabama, Birmingham, AL, USA) or no insert, and 375 ng of the pRL *Renilla* luciferase reporter vector. Two days after transfection, cells were lysed with Passive Lysis Buffer (Promega, Madison, WI, USA), and luciferase activity was measured with the Dual-Glo Luciferase Assay System (Promega) and the Synergy H1 Hybrid Multi-Mode Microplate Reader (BioTek, Winooski, VT, USA). Firefly luciferase activity was normalized to *Renilla* luciferase activity.

Western blot analysis

Cells were lysed in NP-40 lysis buffer, and Western blot analysis was performed according to standard protocols. The following primary antibodies were used: hemagglutinin (HA; 1:1000; Covance, Princeton, NJ, USA), KDM5A (1:1000; Abcam, Cambridge, United Kingdom), GFAP (1:500; Millipore-Sigma), galactosylceramidase (1:500; Millipore-Sigma), tubulin β3 class III (TUBB3) (TuJ1, 1:2000; Millipore-Sigma), notch intracellular domain (NICD) (Val1744, 1:1000), eIF4E (1:2000), phospho-eIF4E (Ser209, 1:1000), ERK 1/2 (1:4000), phospho-ERK1/2 (Thr202/Tyr204, 1:4000), STAT3 (1:2000), phospho-STAT3 (Tyr705, 1:2000) (Cell Signaling Technology), and GAPDH (1:1000; Santa Cruz Biotechnology, Santa Cruz, CA, USA). Secondary antibodies were horseradish peroxidase–conjugated goat anti-mouse and anti-rabbit IgG (1:5000; Santa Cruz Biotechnology).

Immunocytochemistry

Immunocytochemical analyses were performed as described (24). Cells were fixed (30 min) with 4% paraformaldehyde (USB Products; Cleveland, OH, USA) and blocked (30 min) with 5% normal goat serum (Millipore-Sigma) and 0.2% Triton X-100 (Amresco, Cleveland, OH, USA). Afterward, the cells were incubated (1 h) with antibodies against green fluorescent protein (GFP) (1:500; Thermo Fisher Scientific), and GFAP (1:1000; Dako, Copenhagen, Denmark), followed by secondary antibodies conjugated to Alexa Fluor 488 (goat anti-mouse IgG, 1:1000; Thermo Fisher Scientific) or Cy3 (goat anti-rabbit IgG, 1:1000; Jackson ImmunoResearch, West Grove, PA, USA) for 30 min. Cell nuclei were stained with DAPI (Millipore-Sigma). Images were obtained with an inverted fluorescence microscope (DMIL; Leica, Wetzlar, Germany).

Chromatin immunoprecipitation

Chromatin immunoprecipitation (ChIP) was performed as described elsewhere (5), with some modifications. Cells were cross-linked (10 min) with 1% formaldehyde and then harvested before being lysed in lysis buffer. The cross-linked chromatin was sonicated to obtain DNA fragments of 0.5–1 kb using the Vibra-Cell VCX 500 ultrasonic processor (Sonics and Materials, Newtown, CT, USA), and 1% of each sample was saved as input. Chromatin was incubated (overnight, 4°C) with 2 μg of antibodies against KDM5A (Abcam), H3K4me3 (Millipore-Sigma), H3K9me2 (Active Motif, Carlsbad, CA, USA), and normal rabbit IgG (Santa Cruz Biotechnology), before being incubated for 2 h with protein A-agarose beads (Millipore-Sigma). After extensive washing, the immune complexes were eluted, and the cross-linking was reversed *via* incubation (overnight, 65°C) in 200 mM NaCl. The reverse cross-linking and all subsequent steps were also performed on the 1% input sample. DNA was recovered with the QiaQuick PCR Purification Kit (Qiagen) and subjected to real-time PCR analysis with the appropriate primer sequences (Supplemental Table S2).

MicroRNA prediction

Candidate microRNAs (miRNAs) that target the *Kdm5a* 3′-UTR, and their potential binding sites, were predicted using miRNA target software prediction tools, including TargetScan (*http://www.targetscan.org*), miRANDA (*http://www.microrna.org*), and RNAhybrid (*http://bibiserv.techfak.uni-bielefeld.de/rnahybrid/submission.html*).

Detection of miRNA expression

The miScript PCR system (Qiagen) was used to analyze miRNA expression, according to the manufacturer's instructions. Total RNA was isolated from cells using the Trizol reagent, and cDNA was generated from 2 μg of this using the miScript II RT kit. Real-time PCR was performed with the miScript SYBR Green PCR kit, *via* 6 miScript Primer Assays comprising Rn_miR-9_1, Rn_miR-29a*_2, Rn_miR-124*_1, Rn_miR-181a_2, Rn_miR-181c_2, and Hs_RNU6-2_11. PCR cycling consisted of 95°C for 15 min, followed by 40 cycles of 94°C for 15 s, 55°C for 30 s, and 70°C for 30 s. Results were normalized to U6 small nuclear RNA (RNU6) expression.

Construction of 3′-UTR reporter plasmids and the luciferase assay

Predicted target regions in the rat *Kdm5a* 3′-UTR (NM_001277177.1), comprising R1 (bases 5491–6031, length 541 bp), R2 (bases 6422–7036, length 615 bp), R3 (bases 7396–8027, length 632 bp), R4 (bases 8677–9249, length 573 bp), and R5 (bases 9265–9928, length 664 bp) were amplified by PCR with appropriate primers (Supplemental Table S3) and cloned into the *Eco*RI/*Pst*I sites of a pGL3UC luciferase reporter vector (25). HEK293T cells were cotransfected with 400 ng of the MDH1-PGK-GFP 2.0 expression vector (kindly provided by Dr. Chen, Achelois Pharmaceuticals, Chapel Hill, NC, USA) containing either precursor miRNAs (*premiR-9*, *premiR-124*, *premiR-181a*, and *premiR-181c*) or no insert (negative control), 50 ng of firefly luciferase plasmids harboring the *Kdm5a* 3′-UTR, and 10 ng of the pRL *Renilla* luciferase reporter vector, using Lipofectamine 2000. Two days after transfection, a luciferase assay was performed as previously described.

miRNA overexpression by nucleofection

NPCs were nucleofected with 10 μg of either MDH1-PGK-GFP 2.0 expressing *premiR-9*, *premiR-124*, *premiR-181a*, or *premiR-181c*, or empty vector (negative control), using the Amaxa 4D-Nucleofector System (Lonza), as previously described.

Statistical analysis

Results are expressed as means ± SEM or SD. Statistical significance was determined with the Student's *t* test, with significance set at $P < 0.05$ *vs.* control.

RESULTS

KDM5A represses *Gfap* expression in neural progenitor cells

To investigate the role of KDM5A, KDM5B, and KDM5D in NPC fate determination, we designed control and KDM5

subfamily-specific siRNAs (**Fig. 1*A***). NPCs proliferate in the presence of EGF, FGF2, or both and differentiate into neurons, astrocytes, and oligodendrocytes when mitogens are absent (26). After NPCs derived from E14 rat cortex were expanded for 1 wk in the presence of EGF and FGF2, cells were dissociated, and each siRNA was introduced to the NPCs *via* nucleofection. The NPCs were expanded for an additional 2 d in the presence of mitogens, then mRNAs were harvested and subjected to real-time RT-PCR analysis. Knockdown of KDM5A during NPC expansion increased the expression of the astroglial gene *Gfap*, without affecting the transcription of oligodendrocyte marker gene oligodendrocyte transcription factor 2 (*Olig2*), neuronal gene *Tubb3*, and the NSC marker gene Nestin (*Nes*) (Fig. 1*B*). This result suggests that KDM5A represses astrocyte differentiation in NPCs and secures NPCs to expand as NPCs. The other KDM5 family subtypes did not exert any effect on NPC fate, emphasizing the specific role of KDM5A in NPC maintenance.

We next performed luciferase assays to confirm the repression of astrocyte differentiation by KDM5A during NPC expansion. When cells were cotransfected with a vector containing HA-tagged KDM5A, and a luciferase vector containing the *Gfap* promoter sequence (−2163 to +47), the resultant luciferase activity was significantly reduced compared to that exhibited by the luciferase vector with empty backbone vector (pcDNA3)–transfected control cells (Fig. 1*C*, *D*). In addition, introduction of NPCs with *Kdm5a* siRNA increased GFAP expression at the protein level, as demonstrated by Western blot analysis (Fig. 1*E*). Similarly, nucleofection of NPCs with *Kdm5a* siRNA, and a GFP vector, resulted in the visualization of a significantly higher number of GFP^+ astrocytes than control siRNA transduced NPCs, as assessed by immunocytochemistry (Fig. 1*F*, *G*). These data clearly suggest that KDM5A represses astrocytogenesis in NPCs.

KDM5A represses astrocytogenesis by preventing H3K4 methylation on the *Gfap* promoter

To explore the role of KDM5A during astrocytogenesis, we designed primers to perform ChIP on the *Gfap* promoter (**Fig. 2*A***). Primers designated as P1 [−2165 to −2063, containing the potential KDM5A biding site CCGCCC (27)], P2 (−1520 to −1420, including a known STAT binding site), P3 (−1141 to −994), and P4 [−99 to +13, containing the transcription start site (TSS)(28)], were used for the experiment. We decided to compare the H3K4 methylation levels between NPCs, and cells induced to differentiate into astrocytes; therefore, the NPCs were dissociated, plated, and exposed to CNTF (in the absence of growth factors) to facilitate astroglial differentiation. Control NPCs were treated according to the same protocol, but were exposed to EGF/FGF2 without CNTF. The results showed that CNTF-treated differentiated cells exhibited 5000-fold greater *Gfap* transcript level than that displayed by control NPCs (Fig. 2*B*). When ChIP was performed under the same conditions, we detected an upregulation of H3K4 trimethylation in CNTF-treated cells that was localized to the regions detected by P3 and P4 (Fig. 2*C*). We observed that KDM5A occupancy on the *Gfap* promoter was reduced in the regions analyzed by P1–P3 and significantly reduced in the region detected by P4 (Fig. 2*D*). These data suggest that KDM5A is recruited to the *Gfap* promoter when NPCs are cultured with growth factors, but diminishes when NPCs differentiate into astrocytes.

To confirm the role of KDM5A in the repression of astrocytogenesis in NPCs, we knocked down KDM5A using siRNA. For this analysis, the NPCs were dissociated, plated, and cultured in the presence of EGF and FGF2, to induce proliferation. KDM5A knockdown resulted in significantly less recruitment of KDM5A to the *Gfap* promoter in the P1 and P4 regions (Fig. 2*E*). In addition, KDM5A knockdown significantly upregulated H3K4 trimethylation (Fig. 2*F*), and reduced H3K9 dimethylation (Fig. 2*G*) in the P4 region of the *Gfap* promoter. These data suggest that KDM5A is a key histone demethylase that represses astrocyte differentiation in NPCs by preventing H3K4 methylation.

Kdm5a mRNA expression is high, but KDM5A protein production is low during NPC differentiation

Because KDM5A repressed astrocyte differentiation in NPCs, we hypothesized that KDM5A levels would be reduced once repression of astrocytogenesis was no longer needed after differentiation. Thus, we compared *Kdm5a* transcript expression levels between NPCs and cells induced to differentiate into astrocytes by CNTF treatment. Contrary to our hypothesis, we observed higher *Kdm5a* mRNA expression levels in CNTF-treated differentiated cells than in NPCs (**Fig. 3*A***). However, when the protein expression levels between the two conditions were examined by Western blot analysis, we found that the KDM5A protein levels were lower in the differentiated cells compared to the NPCs (Fig. 3*B*). These data clearly indicate that, as hypothesized, KDM5A protein levels are low after differentiation, but that *Kdm5a* mRNA expression does not correlate with this observed reduction in protein production.

KDM5A protein expression is not regulated by protein degradation

To explore how this discrepancy occurs, we first decided to use MG132 and BTZ to inhibit protein degradation and test the hypothesis that KDM5A degradation by the proteasome may enable the observed persistence of high *Kdm5a* expression levels, while reducing KDM5A levels. NICD was used as a control to validate the effectiveness of the inhibitors, and as expected, MG132 treatment dramatically upregulated NICD protein expression in both NPCs and CNTF-treated cells (Fig. 3*C*). However, we did not observe that MG132 treatment caused any increase in the level of KDM5A protein expression in CNTF-treated differentiated cells compared to NPCs (Fig. 3*C*). Neither did repetition of the experiment with BTZ

induce any increase in KDM5A levels (Fig. 3*D*), suggesting that KDM5A protein expression is not affected by protein degradation.

KDM5A protein expression is not regulated by miRNAs

We next explored whether miRNAs are involved in the observed discrepancy between *Kdm5a* expression and the KDM5A protein level. First, we predicted the *Kdm5a* 3′-UTR for miRNA binding sites using the TargetScan, miRANDA, and RNAhybrid software programs. We identified several miRNA binding sites for *miR-9*, *miR-29a*, *miR-181a,c*, and *miR-124* (**Fig. 4*A***). To determine whether the expression levels of these miRNAs are altered during NPC differentiation, we divided the NPCs into 2 groups, treating the first with EGF and FGF2 to maintain cells as NPCs and facilitate proliferation, and the second with CNTF (in the absence of growth factors) to induce differentiation for 24 h. Then cells were harvested, their total RNA was isolated, and the expression of the miRNAs of interest was detected by real-time PCR, for which the RNU6 was used as a loading control. The results of this analysis showed that, during differentiation, *miR-9*, *miR-124*, *miR-181a*, and *miR-181c* expression was significantly up-regulated (Fig. 4*B*), suggesting that during or after differentiation, these highly up-regulated miRNAs may bind to the *Kdm5a* 3′-UTR and repress KDM5A translation. To test this hypothesis, we performed a luciferase assay that determines the levels of transcripts affected by miRNAs binding to 3′-UTR. In detail, a single *Kdm5a* 3′-UTR miRNA binding region (*i.e.*, one of the regions R1–R5; Supplemental Fig. S2*A*) was cloned into the firefly luciferase 3′-UTR in a pGL3UC luciferase reporter vector. If a miRNA binding to the region affected the stability of

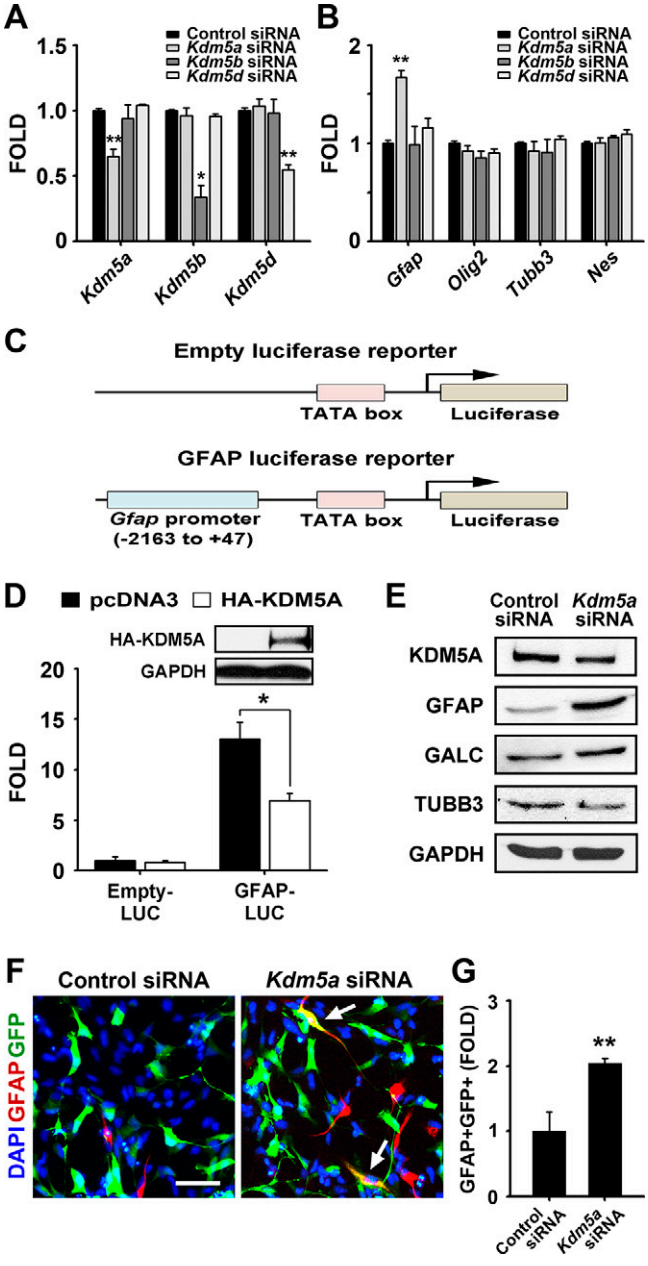

Figure 1. KDM5A suppresses astrocyte differentiation in rat fetal NPCs. *A*) The specificity of *Kdm5a*, *Kdm5b*, and *Kdm5d* siRNA in NPCs was validated by real-time PCR. NPCs were nucleofected with *Kdm5a*, *Kdm5b*, *Kdm5d*, or control siRNA, and cells were cultured in the presence of EGF and FGF2 for 2 d. *Kdm5a*, *Kdm5b*, and *Kdm5d* mRNA expression levels were normalized to that of *Gapdh*,, and compared between siRNA-treated and control NPCs. *B*) *Gfap*, *Olig2*, *Tubb3*, and *Nes* mRNA expression levels were determined by real-time PCR. NPCs were nucleofected with *Kdm5a*, *Kdm5b*, *Kdm5d*, or control siRNA, and then cultured for 2 d in the presence of growth factors. mRNA expression levels were normalized to that of *Gapdh* and compared between siRNA-treated and control NPCs. Results are expressed as means ± SEM of results of 3 independent experiments. $*P < 0.05$, $**P < 0.01$ (Student's *t* test). *C*) Luciferase reporter constructs. The GFAP luciferase reporter construct comprises a human *Gfap* promoter fragment (−2163 to +47) inserted into the pGL3-Basic vector (empty luciferase reporter construct). *D*) Relative luciferase activity was measured 2 d after cotransfection of HEK293T cells with pcDNA3-HA-KDM5A or empty-pcDNA3, with the firefly GFAP luciferase-reporter (GFAP-LUC) or empty luciferase-reporter (Empty-LUC) construct, and the *Renilla* luciferase reporter vector. Firefly luciferase activity was normalized to *Renilla* luciferase activity, and then to activity exhibited by cells that were cotransfected with pcDNA3 and Empty-LUC. Data represent means ± SEM of the results of 3 independent experiments. $*P < 0.05$ (Student's *t* test). KDM5A levels in HEK293T cells transfected with GFAP-LUC and either the pcDNA3-HA-KDM5A or pcDNA3 vector were determined by Western blot analysis (2 d after transfection) (top). GAPDH was used as a loading control. *E*) KDM5A, GFAP, GALC, TUBB3, and GAPDH levels in NPCs nucleofected with either *Kdm5a* or control siRNA, and cultured (3 d) in the presence of EGF and FGF2, were determined by Western blot analysis. GAPDH was used as the loading control. *F*) Immunocytochemical data showing GFAP (red), GFP (green), and DAPI nuclear staining (blue) in NPCs nucleofected with either *Kdm5a* or control siRNA with the pmaxGFP vector and cultured (3 d) in the presence of mitogens. Arrows: GFAP/GFP double-positive cells. Scale bar, 50 μm. *G*) Quantitative analysis of GFAP/GFP double-positive cells among the total GFP-positive cells. The number of GFAP/GFP-positive cells detected in *Kdm5a* siRNA-treated NPCs was divided by that of control siRNA-treated NPCs. Data represent means ± SEM of results of 3 independent experiments. $**P < 0.01$ (Student's *t* test).

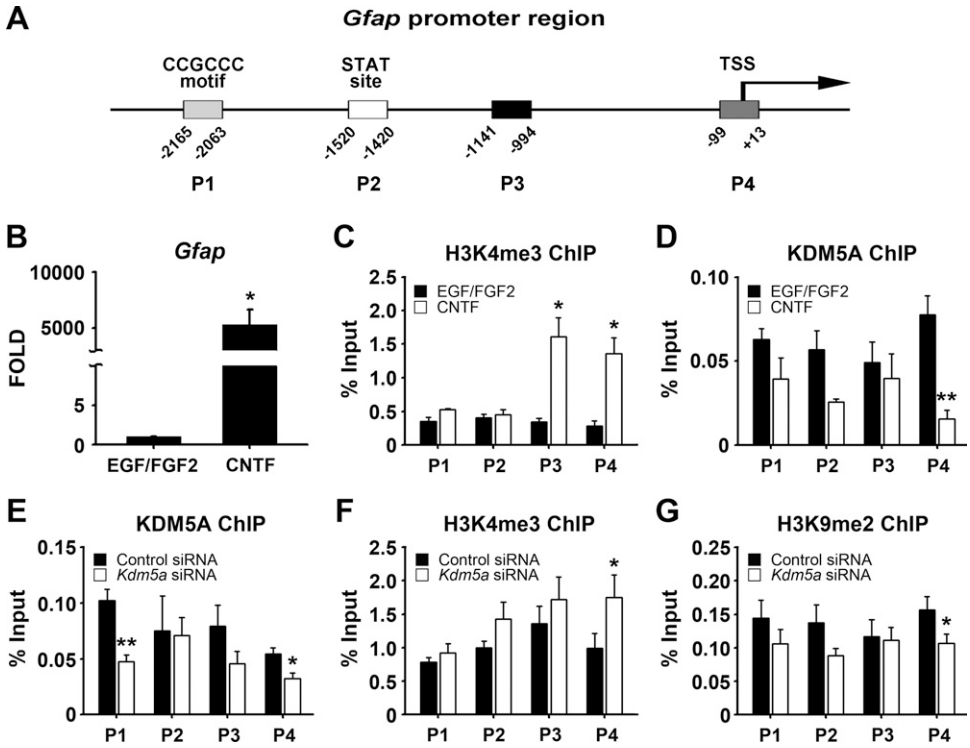

Figure 2. KDM5A is recruited to the *Gfap* promoter during proliferation and reduces the H3K4me3 level. *A*) Primers designed for the *Gfap* promoter regions. P1 includes the predicted KDM5A binding motif (CCGCCC), P2 contains a STAT binding site, P3 comprises a randomly selected site around position −1000, and P4 contains the TSS. *B*) *Gfap* expression was evaluated by real-time RT-PCR. NPCs were cultured (24 h) in the presence of EGF/FGF2, or CNTF without EGF/FGF2. *Gapdh* was used as the internal control. Data represent means ± SEM of results of 3 independent experiments. $*P < 0.05$ (Student's *t* test). *C*, *D*) ChIP analysis of H3K4me3 (*C*) and KDM5A (*D*) levels in the *Gfap* promoter regions (P1–4) in NPCs cultured (12 h) with EGF/FGF2 or CNTF only. Enrichment relative to input is shown as means ± SEM of results in 3 independent experiments. $*P < 0.05$, $**P < 0.01$ (Student's *t* test). *E–G*) ChIP analysis of KDM5A (*E*), H3K4me3 (*F*), and H3K9me2 (*G*) levels in the *Gfap* promoter regions (P1–4) in NPCs nucleofected with either *Kdm5a* or control siRNA, then cultured (2–3 d) in EGF/FGF2. Enrichment relative to input is shown as means ± SEM ($n = 3$, *E*; $n = 5$, *F*, *G*). $*P < 0.05$, $**P < 0.01$ (Student's *t* test).

luciferase transcripts, reduced luminescence value would be detected due to the low levels of luciferase production. HEK293T cells were cotransfected with this reporter vector along with a miRNA-GFP expression vector (MDH1-PGK-GFP 2.0) containing one of the highly up-regulated miRNAs or no insert (control) and a *Renilla* luciferase reporter vector. After 48 h, the cells were lysed, and their luciferase activity was measured. Despite overexpression of miR-9, miR-124, and miR-181c, we did not observe a resultant decrease in luciferase activity compared with that exhibited by control cells (Supplemental Fig. S2*B–D*). This result suggests that although the analyzed miRNAs are up-regulated during differentiation, they do not repress KDM5A translation. Overexpression of miR-181a showed subtle but significant reduction (23%) of luciferase activity (Supplemental Fig. S2*E*). Thus, to verify this result in NPCs, we evaluated KDM5A protein expression levels after miR-9, miR-124, miR-181a, and miR-181c overexpression, and showed that ectopic expression of each of these miRNAs, even miR-181a, failed to repress KDM5A expression levels (Fig. 4*C*). Together, these data suggest that the observed discrepancy between *Kdm5a* mRNA and KDM5A protein levels does not result from miRNA activity.

KDM5A translation is regulated by the translational machinery

To further explore the mechanism underlying the observed discrepancy between *Kdm5a* mRNA and KDM5A protein expression in the CNTF-treated differentiated cells, we next assessed whether NPC translation activity is altered during differentiation. We conducted a Western blot analysis to detect changes in eIF4E expression and phosphorylation levels during astrocyte differentiation. CNTF treatment induced STAT3 phosphorylation and markedly reduced KDM5A protein expression (**Fig. 5*A***). In addition, the phosphorylation levels of both eIF4E and its upstream kinase ERK1/2 were reduced compared with those exhibited by control NPCs. These data suggest that during astrocytogenesis, the level of translational activity is reduced compared to that occurs during NPC proliferation. To confirm whether KDM5A translation is affected by this modulation of translational activity, we treated NPCs with Cerco, a MNK1/2 (*i.e.*, ERK1/2 substrate, which is known to phosphorylate eIF4E) and translation inhibitor. Three days of Cerco (5 μM) treatment of NPCs in the presence of mitogens showed a reduced level of eIF4E phosphorylation, and also decreased KDM5A and increased GFAP protein expression, respectively (Fig. 5*B*). In addition, real-time PCR results revealed that Cerco treatment during NPC proliferation dramatically increased *Gfap* but did not alter *Kdm5a mRNA* expression (Fig. 5*C*). Similarly, the conducted immunocytochemical analysis revealed a significant increase in the number of $GFAP^+$ astrocytes by Cerco, compared with vehicle (DMSO)-treated control cells (Fig. 5*D*, *E*). These data suggest that inhibition of MNKs and eIF4E phosphorylation reduces KDM5A protein production while not affecting the *Kdm5a* mRNA expression and results in astrocytogenesis. Upon treatment of NPCs with U0126, a MEK 1/2 inhibitor, in the presence of EGF and FGF2, we

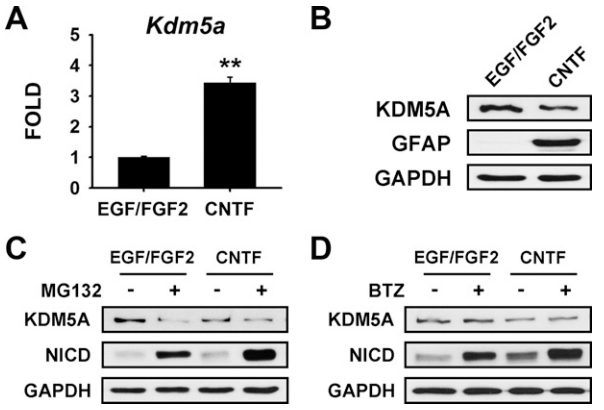

Figure 3. The increased *Kdm5a* transcript and decreased KDM5A protein expression during astrocyte differentiation is not caused by protein degradation. *A*) Relative *Kdm5a* levels were measured by real-time RT-PCR in NPCs cultured with EGF/FGF2 or CNTF only for 24 h. *Gapdh* was used as the internal control, and mRNA levels of EGF/FGF2-treated cells were set to 1. All values represent means ± SEM of results in 3 independent experiments. $^{**}P < 0.01$ (Student's *t* test). *B*) KDM5A and GFAP protein levels in NPCs cultured for 24 h with EGF/FGF2 or CNTF were determined by Western blot analysis. GAPDH was used as the loading control. *C*, *D*) Western blot analysis of KDM5A and NICD levels in NPCs cultured for 24 h in EGF/FGF2 or CNTF only, and treated with either 5 μM MG132 (*C*), or 25 nM BTZ (*D*) for 6 h before lysis. NICD was used as a positive control for proteasome inhibition, and GAPDH was used as the loading control.

also observed reduction in the level of phosphorylation of ERK1/2 and eIF4E, and a decrease and increase in the expression of KDM5A and GFAP, respectively (Fig. 5*F*). U0126 treatment during NPC proliferation also dramatically induced *Gfap* and *Tubb3* mRNA and reduced *Nes* expression (Fig. 5*G*). Together, these data suggest that MNK inhibition is sufficient to inhibit KDM5A translation and induce astrocytogenesis and that abrogation of upstream MEK1/2 signaling also reduces translation activity, thereby inducing NPC differentiation to astrocytes.

DISCUSSION

The precise regulation of gene expression is critical for normal development, and for the prevention of disease progression. It is achieved *via* various mechanisms, including histone modification. In the present study, we demonstrated that the histone modifier KDM5A is necessary for repression of GFAP expression in NPCs derived from the E14 rat cortex. KDM5A has been reported to exert enzyme activity against H3K4me2 and H3K4me3 (11). In contrast to histone acetylation, whose effects correlate with gene activation, the effect of histone methylation is dependent upon the identity of the modified lysine residues (29). For example, methylation of H3K4, K36, and K79 is associated with transcriptional activation, while that of H3K27 and H4K20 is associated with gene repression. Thus, by controlling gene expression, it seems plausible that histone demethylases are involved in cell fate determination. Indeed, recent evidence has shown that histone demethylases regulate stem cell fate control (5–7, 30, 31). For example, JMJD3/KDM6B activates specific components of the neurogenic program by removing H3K27me3 repression marks (5). Inhibition of KDM5B has been reported to enhance neural and neuronal development (7, 30). In addition, the specific inhibition of LSD1/KDM1A has been shown to induce the suppression of neurogenesis in human fetal NSCs (6). These suggest that KDM family members have specific target genes and that their regulation of histone methylation is a critical mechanism that enables precise control of gene expression.

Our data suggest that KDM5A is essential for the repression of *Gfap* transcription during NPC proliferation by binding to the *Gfap* promoter, and demethylating H3K4. In doing so, KDM5A inhibits differentiation, and ensures that NPCs retain the ability to proliferate in the presence of EGF and FGF2. The correct and precise regulation between self-renewal/proliferation and differentiation is critical in NPCs and NSCs. The results of our study suggest that one of the normal functions of KDM5A is to maintain optimal epigenetic conditions to enable cell proliferation, and to prevent differentiation. This conclusion is supported by recent reports that used different cell lines to reveal the involvement of KDM5A in the survival of drug-resistant cancer cells (12, 14). The authors developed an inhibitor, CPI-455, that was selective for KDM5A. Treatment of cells with the inhibitor increased drug-resistant cancer-cell death, suggesting that KDM5A indeed contributes to the survival and proliferation of cancer cells (12). In our study, treatment of a KDM5A inhibitor also increased astrocytogenesis (data not shown) suggesting the importance of

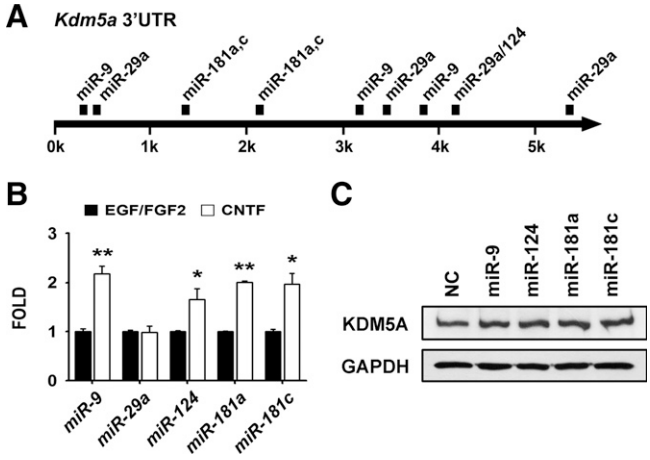

Figure 4. The discrepancy between *Kdm5a* and KDM5A expression in NPCs does not result from miRNAs activity. *A*) Schematic diagram of predicted miRNA binding sites in the *Kdm5a* 3′UTR. *B*) After expansion (1 wk) in EGF and FGF2, NPCs were dissociated, plated, and cultured (24 h) with EGF/FGF2 or CNTF only, before miRNA expression levels were determined by real-time PCR. RNU6 was used as the loading control. Data represent means ± SEM of results in 3 independent experiments. $^{*}P < 0.05$, $^{**}P < 0.01$ (Student's *t* test). *C*) Western blot analysis of KDM5A expression in NPCs nucleofected with the MDH1-PGK-GFP 2.0 vector expressing *miR-9*, *miR-124*, *miR-181a*, *miR-181c*, or no insert (negative control, NC), and cultured for 3 d in EGF and FGF2. GAPDH served as the loading control.

demethylation in the repression of the *Gfap* promoter. Another report (32) showing that KDM5A knockdown in pRB-deficient cells restores mitochondrial genes that most likely play critical roles in myogenesis is very similar to the data generated by the NPC system used in the present study, which demonstrate that KDM5A prevents astrocytogenesis. The same research group also performed a genome-wide analysis that identified a range of KDM5A target genes, most of which were divided into 2 classes: comprising differentiation-independent genes encoding mitochondrial proteins and differentiation-dependent, cell cycle-related genes (17). According to the data produced in that report and in the present study, KDM5A appears to have the ability to bind to genes that regulate differentiation, and to inhibit their transcription by removing H3K4 methylation to facilitate proliferation. Interestingly, the regulation of differentiation-independent target genes that encode mitochondrial proteins, by treatment with metformin, phenformin, rotenone, or sodium azide (mitochondrial respiratory chain complex I or V inhibitors), has been shown to lead to reduced myogenesis (32). This finding suggests that correct mitochondrial function which can be modulated by KDM5A is also essential for myogenic differentiation and again supporting the hypothesis that KDM5A function is a key epigenetic mechanism underlying the negative regulation of differentiation. A similar demonstration that KDM5A upregulation during osteoporosis impairs the ability of bone morphogenetic protein 2 to promote osteogenic differentiation also supports the view that KDM5A inhibits differentiation (33).

In the present study, by performing ChIP, we observed that KDM5A binds to the CCGCCC motif and TSS of the *Gfap* promoter. Other researchers have reported similar results that show that KDM5A preferentially binds to proximal promoter sites (17). The CCGCCC motif has been identified, and an AT-rich interaction domain of KDM5A is thought to mediate KDM5A binding to the DNA in which the CCGCCC sequence is embedded (27). Because KDM5A is known to interact with many partner proteins, including the pRB family, TATA-binding protein, and a repressor of erythroid developments, KDM5A binding sites of DNA can be different depending on the identity of binding partner, as well as on the cellular context (17, 34–36). In the present study, we observed reduced KDM5A binding to both the CCGCCC motif and TSS

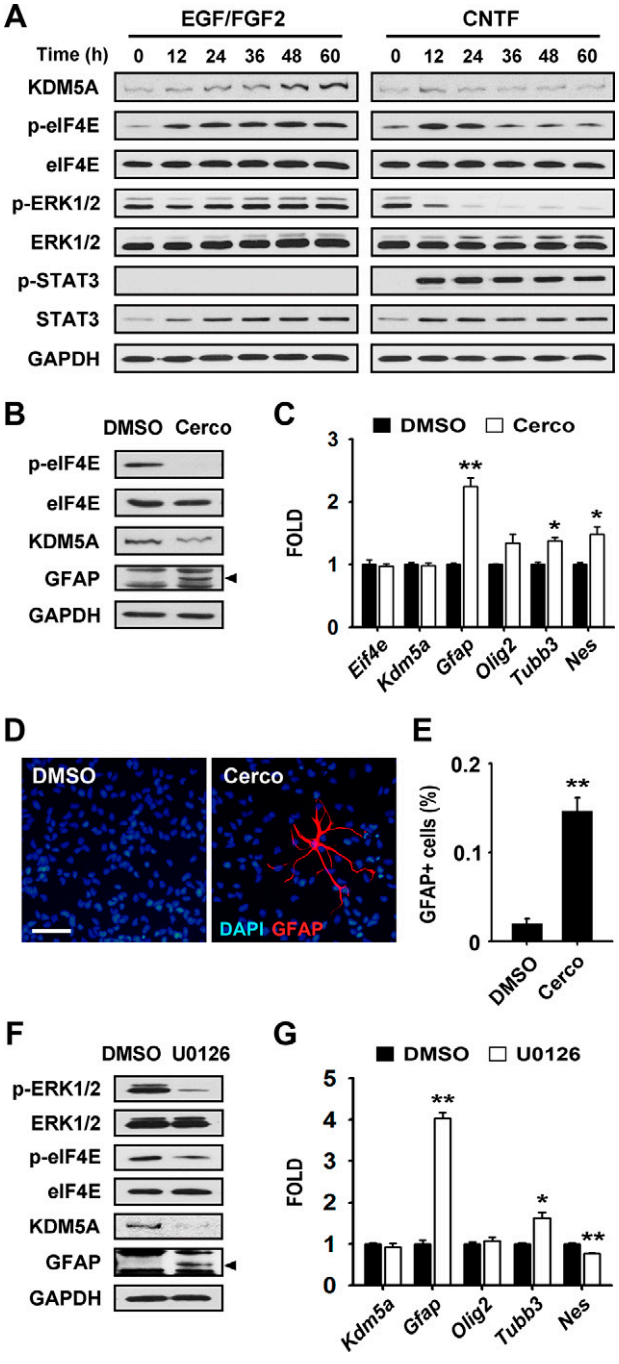

Figure 5. KDM5A translation is reduced during astrocytogenesis. *A*) Western blot analysis of KDM5A, p-eIF4E (Ser209), total eIF4E, p-ERK1/2 (Thr202/Tyr204), total ERK1/2, p-STAT3 (Tyr705), total STAT3, and GAPDH in NPCs cultured with EGF/FGF2 or CNTF only for the indicated periods. *B*) p-eIF4E, total eIF4E, KDM5A, GFAP, and GAPDH levels in NPCs were detected by Western blot analysis 3 d after treatment with 5 μM Cerco or DMSO (vehicle), in the presence of growth factors. *C*) *Eif4e*, *Kdm5a*, *Gfap*, *Olig2*, *Tubb3*, and *Nes* mRNA levels were measured by real-time PCR in NPCs cultured for 2 d with 5 μM Cerco or DMSO, in the presence of EGF/FGF2. The expression level of each mRNA was normalized to that of *Gapdh*. mRNA expression levels in DMSO-treated cells was set as 1. Data represent means ± SEM of results in 3 independent experiments. $*P < 0.05$, $**P < 0.01$ (Student's *t* test). *D*) Representative photomicrographs of NPCs treated 4 d with 5 μM Cerco or DMSO, in the presence of EGF/FGF2. Cells were immunostained for GFAP (red) and DAPI stained nuclei (blue). Scale bar, 50 μm. *E*) Quantitative analysis of astrocytes. The number of $GFAP^+$ cells was divided by that of $DAPI^+$cells. All values represent means ± SEM of results in 3 independent experiments. $**P < 0.01$ (Student's *t* test). *F*) p-ERK1/2, total ERK1/2, p-eIF4E, total eIF4E, KDM5A, and GFAP levels were assessed by Western blot analysis. NPCs were treated for 2 d with 50 μM U0126 or DMSO, in the presence of mitogens. GAPDH was used as the loading control. *G*) *Kdm5a*, *Gfap*, *Olig2*, *Tubb3*, and *Nes* expression was assessed by real-time PCR in NPCs cultured (2 d) with 50 μM U0126 or DMSO, in the presence of growth factors. mRNA expression in DMSO-treated cells was set as 1. Data represent means ± SEM of results in 3 independent experiments. $*P < 0.05$, $**P < 0.01$ (Student's *t* test).

when KDM5A was knocked down; however, the levels of H3K4me3 were correspondingly upregulated only at the TSS, but not in the region containing the CCGCCC motif. Thus, it is likely that KDM5A occupancy on the *Gfap* promoter during NPC proliferation represses astrocytogenesis by demethylating H3K4 at the TSS.

The results generated in the present and in previously published studies clearly suggest that KDM5A functions to maintain cells in an undifferentiated state, and to facilitate cellular proliferation (12, 14, 17, 32, 33). Thus, the precise control of both KDM5A expression and activity is critical for normal development and prevention of disease. Since KDM5A maintains the NPC state by preventing the spontaneous differentiation of NPCs to astrocytes, we hypothesized that KDM5A levels would be higher in NPCs than CNTF-treated differentiated cells; however, we unexpectedly detected significantly higher *Kdm5a* transcripts, but significantly lower KDM5A protein levels in CNTF-treated cells than NPCs. We postulated that this discrepancy between *Kdm5a* and KDM5A levels during differentiation could be caused by *1*) proteasome-mediated KDM5A degradation following *Kdm5a* transcription and translation; *2*) improper *Kdm5a* translation resulting from miRNAs specifically expressed during differentiation; or *3*) inhibition of KDM5A translation during differentiation. When we tested hypotheses 1 and 2, neither protein degradation nor miRNAs were involved in the regulation of KDM5A expression.

Instead, KDM5A protein expression appears to be regulated by the translational machinery. The antifungal agent Cerco has recently been identified as an MNK inhibitor (37). As discussed, NPCs proliferate in the presence of growth factors, and differentiate in the absence of mitogens. Growth factors such as EGF and FGF2 activate MAPK signaling, including the downstream signaling components, MNKs (38). In the presence of growth factors, we observed phosphorylation of both ERK1/2 and the MNK substrate, eIF4E. Treatment of cells with the MNKs inhibitor Cerco in the presence of EGF and FGF2 resulted in reduced p-eIF4E levels; however, we also unexpectedly observed that Cerco treatment induced a remarkable reduction and increase in KDM5A and GFAP levels, respectively. This suggests that MNK inhibition affects the induction of astrocytogenesis by the regulation of KDM5A protein expression. Our results also suggest that *Kdm5a* mRNA translation correlates with MNK activation and eIF4E phosphorylation. For the translation to initiate, eIF4E specifically recognizes 5′ mRNA cap (m7G) as a cap-binding subunit of eIF4F complex which also contains the RNA helicase eIF4A and the scaffolding protein eIF4G (20, 39). Although the exact role of eIF4E phosphorylation in translation is not understood clearly, similar to ours, other studies have found that eIF4E phosphorylation is positively correlated with the translation rate (40, 41). In addition, a recent study revealed the importance of eIF4E phosphorylation in the translational upregulation of a subset of mRNAs implicated in tumorigenesis (42). When Ser209, the only eIF4E residue phosphorylated by MNKs, was substituted by alanine and introduced to mouse embryonic fibroblasts to generate a knock-in system, the cells were resistant to oncogene-induced transformation. Likewise, another recent study showed the essential role of MNK1 in the brain-derived neurotrophic factor–stimulated translation of proteins that are involved in neurotransmission and synaptic plasticity (43). These studies verify the important role of MNKs and phospho-eIF4E in a subset of gene translation. However, the crystal structure analysis, and subsequent biophysical studies of eIF4E-binding to m7G have revealed that the binding affinity of phosphorylated eIF4E to capped mRNA is less than that of nonphosphorylated eIF4E (44). Although this observation renders it difficult to elucidate the exact role of eIF4E phosphorylation in translation, it has been speculated that phosphorylation may enable eIF4E release from the eIF4F complex, thereby facilitating subsequent round of translation (45). When we knocked down eIF4E using siRNA, we observed reduced phosphorylation of eIF4E and KDM5A expression. It also increased GFAP expression (Supplemental Fig. S3). These data indicate that KDM5A expression is truly correlating with the level of eIF4E phosphorylation and regulated by the translational machinery.

It has been known that translation regulation can be affected by several parameters of the 5′-UTR, including its length and the stability of secondary structure, presence of upstream open reading frames, and the levels of GC content, which contribute considerably to determine the amount of protein synthesis from mRNA in a cell (46, 47). The mRNAs that are sensitive to eIF4E mediated translation have generally long 5′-UTR (>300 nt) with high GC content (>60%) and stable secondary structure (free energy < -50 kcal/mol) (47, 48). When we evaluated the 5′-UTR of *Kdm5a*, we found that it has 408 nt, 59.1% GC content, 2 upstream open reading frames, and secondary structure with average free energy of -162.40 kcal/mol (Supplemental Table S4). It has been known that the more structured the 5′-UTR of an mRNA, the more difficult to initiate translation since the scanning ribosomes cannot reach the TSS (46). There are a few genes with mRNA levels that cannot be used as an indicator to predict the protein levels (49–53), and most of which are known to function as transcription factors, proto-oncogenes, growth factors, and so on (47). For example, c-Myc, cyclin D1, ornithine decarboxylase, and vascular endothelial growth factor are proteins that show reduced correlation between the mRNA and protein and are sensitive to eIF4E-mediated translation initiation (49–53). These proteins, similar to KDM5A, have GC rich (>60%) lengthy 5′-UTR with stable secondary structure (Supplemental Table S4), which disturb efficient RNA unwinding by eIF4F complex and unable to load ribosomes (48). KDM5A is also involved in cancer progression, cell proliferation, and cell survival and has specific 5′-UTR features that are known to be regulated by the translational machinery. During or after astrocytogenesis, alteration of eIF4E availability by lack of MEK–ERK–MNK signaling appears to reduce translation of KDM5A. Further research is needed to determine more detailed mechanisms of KDM5A regulation by the translational machinery in NPCs and differentiated cells.

Although very little evidence has been reported yet, regulation of translation can be one of the important checkpoints for the control of stem cell fate. Similar to our

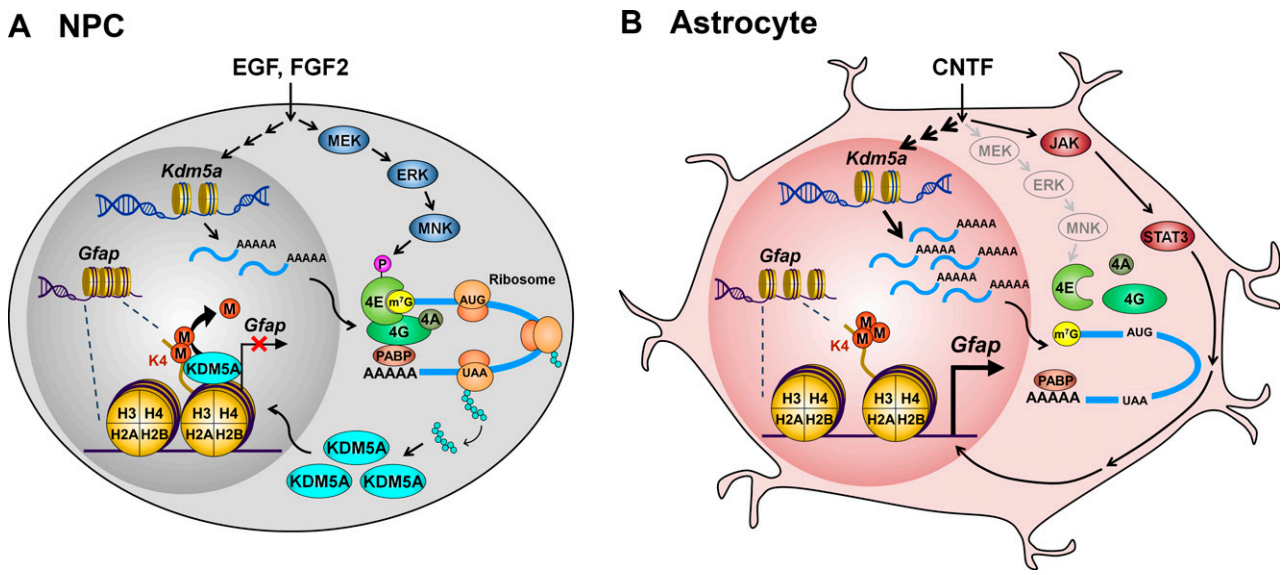

Figure 6. KDM5A function and its expression control in proliferating NPC and differentiating astrocyte. *A*) NPCs proliferate in the presence of EGF and FGF2. The growth factors activate MEK/ERK/MNK signaling pathway that facilitates the phosphorylation of eIF4E, resulting in translation of KDM5A in NPCs. High levels of KDM5A demethylate H3K4 at transcription start site of *Gfap* promoter and repress astrocytogenesis and maintain cells as NPCs. *B*) CNTF induces astrocyte differentiation *via* JAK/STAT3 signaling in NPCs and inhibition of eIF4E mediated translation. During CNTF-induced astrocytogenesis, although *Kdm5a* transcription is up-regulated, its translation is reduced. In the absence of EGF and FGF2, ERK and MNK are no longer activated and subsequently eIF4E phosphorylation is reduced. The KDM5A translation is reduced and consequently, H3K4 methylation retained on *Gfap* promoter promotes transcription of *Gfap* and results in astrocytogenesis from NPCs.

results, which demonstrate that the astrocyte differentiation is repressed by KDM5A and its production is regulated at the translational level, death-associated protein 5 is known to mediate fate determination in human embryonic stem cells and regulate specific sets of proteins that are critical for the transition from pluripotency to differentiation by cap-independent translation (54). This and the data from the present study suggest that stem cell fate can indeed is regulated by translation control. It has also been reported that the brains of patients with fragile X syndrome and those with fragile X mental retardation (FXMR)-1-knockout mice, display elevated eIF4E phosphorylation, and increased matrix metalloproteinase 9 protein levels (55). Genetic and pharmacological reduction of eIF4E phosphorylation has been shown to restore core behavioral deficits and synaptic plasticity in the FXMR system. These data support the importance of eIF4E in translation and brain function, and our results also provide evidence that KDM5A translation is both positively correlated with eIF4E phosphorylation and is essential for the regulation of brain development *via* the maintenance of cell proliferation and the inhibition of cell differentiation.

In summary, the present study shows, for the first time, that KDM5A is a critical epigenetic factor that maintains NPC proliferation and multipotency by repressing astroglial differentiation and that its expression is regulated at the translational level (**Fig. 6**). Our study emphasizes that the regulation of translation is important for normal development to determine cell fate during differentiation. Furthermore, we showed the importance of epigenetic control in regulation of NPC or stem cell fate determination. Our results provide new insights for identifying novel gene targets to regulate stemness or differentiation of NPCs and NSCs. FJ

ACKNOWLEDGMENTS

This research was supported by the Chung-Ang University Excellent Student Scholarship and the National Research Foundation of Korea Grant NRF2017R1A1A1A05000876 (to H.J.K.), funded by the South Korean government. The Alabama Neuroscience Blueprint Core was supported by the U.S. National Institutes of Health, National Institute of Neurological Disorders and Stroke Grants NS39055 and NS057098. The authors declare no conflicts of interest.

AUTHOR CONTRIBUTIONS

H.-J. Kim designed the research, wrote most of the paper, and supervised the research; S.-Y. Kong, W. Kim, and H.-R. Lee performed research and analyzed data; S.-Y. Kong, W. Kim, H.-R. Lee, and H.-J. Kim contributed to discussion of the results and editing the final manuscript.

REFERENCES

1. Gage, F. H. (2000) Mammalian neural stem cells. *Science* **287**, 1433–1438
2. Kim, H. J., McMillan, E., Han, F., and Svendsen, C. N. (2009) Regionally specified human neural progenitor cells derived from the mesencephalon and forebrain undergo increased neurogenesis following overexpression of ASCL1. *Stem Cells* **27**, 390–398
3. Reynolds, B. A., and Weiss, S. (1992) Generation of neurons and astrocytes from isolated cells of the adult mammalian central nervous system. *Science* **255**, 1707–1710
4. Hsieh, J., and Zhao, X. (2016) Genetics and epigenetics in adult neurogenesis. *Cold Spring Harb. Perspect. Biol.* **8**, a018911

5. Jepsen, K., Solum, D., Zhou, T., McEvilly, R. J., Kim, H. J., Glass, C. K., Hermanson, O., and Rosenfeld, M. G. (2007) SMRT-mediated repression of an H3K27 demethylase in progression from neural stem cell to neuron. *Nature* **450**, 415–419
6. Hirano, K., and Namihira, M. (2016) LSD1 mediates neuronal differentiation of human fetal neural stem cells by controlling the expression of a novel target gene, HEYL. *Stem Cells* **34**, 1872–1882
7. Zhou, Q., Obana, E. A., Radomski, K. L., Sukumar, G., Wynder, C., Dalgard, C. L., and Doughty, M. L. (2016) Inhibition of the histone demethylase Kdm5b promotes neurogenesis and derepresses Reln (reelin) in neural stem cells from the adult subventricular zone of mice. *Mol. Biol. Cell* **27**, 627–639
8. Zhang, F., Xu, D., Yuan, L., Sun, Y., and Xu, Z. (2014) Epigenetic regulation of Atrophin1 by lysine-specific demethylase 1 is required for cortical progenitor maintenance. *Nat. Commun.* **5**, 5815
9. Naruse, C., Shibata, S., Tamura, M., Kawaguchi, T., Abe, K., Sugihara, K., Kato, T., Nishiuchi, T., Wakana, S., Ikawa, M., and Asano, M. (2017) New insights into the role of Jmjd3 and Utx in axial skeletal formation in mice. *FASEB J.* **31**, 2252–2266
10. Kooistra, S. M., and Helin, K. (2012) Molecular mechanisms and potential functions of histone demethylases. *Nat. Rev. Mol. Cell Biol.* **13**, 297–311
11. Secombe, J., and Eisenman, R. N. (2007) The function and regulation of the JARID1 family of histone H3 lysine 4 demethylases: the Myc connection. *Cell Cycle* **6**, 1324–1328
12. Vinogradova, M., Gehling, V. S., Gustafson, A., Arora, S., Tindell, C. A., Wilson, C., Williamson, K. E., Guler, G. D., Gangurde, P., Manieri, W., Busby, J., Flynn, E. M., Lan, F., Kim, H. J., Odate, S., Cochran, A. G., Liu, Y., Wongchenko, M., Yang, Y., Cheung, T. K., Maile, T. M., Lau, T., Costa, M., Hegde, G. V., Jackson, E., Pitti, R., Arnott, D., Bailey, C., Bellon, S., Cummings, R. T., Albrecht, B. K., Harmange, J. C., Kiefer, J. R., Trojer, P., and Classon, M. (2016) An inhibitor of KDM5 demethylases reduces survival of drug-tolerant cancer cells. *Nat. Chem. Biol.* **12**, 531–538
13. Horton, J. R., Liu, X., Gale, M., Wu, L., Shanks, J. R., Zhang, X., Webber, P. J., Bell, J. S., Kales, S. C., Mott, B. T., Rai, G., Jansen, D. J., Henderson, M. J., Urban, D. J., Hall, M. D., Simeonov, A., Maloney, D. J., Johns, M. A., Fu, H., Jadhav, A., Vertino, P. M., Yan, Q., and Cheng, X. (2016) Structural basis for KDM5A histone lysine demethylase inhibition by diverse compounds. *Cell Chem. Biol.* **23**, 769–781
14. Sharma, S. V., Lee, D. Y., Li, B., Quinlan, M. P., Takahashi, F., Maheswaran, S., McDermott, U., Azizian, N., Zou, L., Fischbach, M. A., Wong, K. K., Brandstetter, K., Wittner, B., Ramaswamy, S., Classon, M., and Settleman, J. (2010) A chromatin-mediated reversible drug-tolerant state in cancer cell subpopulations. *Cell* **141**, 69–80
15. Benevolenskaya, E. V., Murray, H. L., Branton, P., Young, R. A., and Kaelin, W. G., Jr. (2005) Binding of pRB to the PHD protein RBP2 promotes cellular differentiation. *Mol. Cell* **18**, 623–635
16. Zhao, D., Zhang, Q., Liu, Y., Li, X., Zhao, K., Ding, Y., Li, Z., Shen, Q., Wang, C., Li, N., and Cao, X. (2016) H3K4me3 demethylase Kdm5a is required for NK cell activation by associating with p50 to suppress SOCS1. *Cell Reports* **15**, 288–299
17. Lopez-Bigas, N., Kisiel, T. A., Dewaal, D. C., Holmes, K. B., Volkert, T. L., Gupta, S., Love, J., Murray, H. L., Young, R. A., and Benevolenskaya, E. V. (2008) Genome-wide analysis of the H3K4 histone demethylase RBP2 reveals a transcriptional program controlling differentiation. *Mol. Cell* **31**, 520–530
18. Kong, J., and Lasko, P. (2012) Translational control in cellular and developmental processes. *Nat. Rev. Genet.* **13**, 383–394
19. Siddiqui, N., and Sonenberg, N. (2015) Signalling to eIF4E in cancer. *Biochem. Soc. Trans.* **43**, 763–772
20. Gingras, A. C., Raught, B., and Sonenberg, N. (1999) eIF4 initiation factors: effectors of mRNA recruitment to ribosomes and regulators of translation. *Annu. Rev. Biochem.* **68**, 913–963
21. Proud, C. G. (2015) Mnks, eIF4E phosphorylation and cancer. *Biochim. Biophys. Acta* **1849**, 766–773
22. Bhat, M., Robichaud, N., Hulea, L., Sonenberg, N., Pelletier, J., and Topisirovic, I. (2015) Targeting the translation machinery in cancer. *Nat. Rev. Drug Discov.* **14**, 261–278
23. Kong, S. Y., Park, M. H., Lee, M., Kim, J. O., Lee, H. R., Han, B. W., Svendsen, C. N., Sung, S. H., and Kim, H. J. (2015) Kuwanon V inhibits proliferation, promotes cell survival and increases neurogenesis of neural stem cells. *PLoS One* **10**, e0118188
24. Yoon, H. J., Kong, S. Y., Park, M. H., Cho, Y., Kim, S. E., Shin, J. Y., Jung, S., Lee, J., Farhanullah, Kim, H. J., and Lee, J. (2013) Aminopropyl carbazole analogues as potent enhancers of neurogenesis [published correction in *Bioorg. Med. Chem.* (2014) 22, 927]. *Bioorg. Med. Chem.* **21**, 7165–7174
25. Jin, H., Suh, M. R., Han, J., Yeom, K. H., Lee, Y., Heo, I., Ha, M., Hyun, S., and Kim, V. N. (2009) Human UPF1 participates in small RNA-induced mRNA downregulation. *Mol. Cell. Biol.* **29**, 5789–5799
26. Lee, H. R., Farhanullah, Lee, J., Jajoo, R., Kong, S. Y., Shin, J. Y., Kim, J. O., Lee, J., Lee, J., and Kim, H. J. (2016) Discovery of a small molecule that enhances astrocytogenesis by activation of STAT3, SMAD1/5/8, and ERK1/2 via induction of cytokines in neural stem cells. *ACS Chem. Neurosci.* **7**, 90–99
27. Tu, S., Teng, Y. C., Yuan, C., Wu, Y. T., Chan, M. Y., Cheng, A. N., Lin, P. H., Juan, L. J., and Tsai, M. D. (2008) The ARID domain of the H3K4 demethylase RBP2 binds to a DNA CCGCCC motif. *Nat. Struct. Mol. Biol.* **15**, 419–421
28. Song, M. R., and Ghosh, A. (2004) FGF2-induced chromatin remodeling regulates CNTF-mediated gene expression and astrocyte differentiation. *Nat. Neurosci.* **7**, 229–235
29. Martin, C., and Zhang, Y. (2005) The diverse functions of histone lysine methylation. *Nat. Rev. Mol. Cell Biol.* **6**, 838–849
30. Schmitz, S. U., Albert, M., Malatesta, M., Morey, L., Johansen, J. V., Bak, M., Tommerup, N., Abarrategui, I., and Helin, K. (2011) Jarid1b targets genes regulating development and is involved in neural differentiation. *EMBO J.* **30**, 4586–4600
31. Lambrot, R., Lafleur, C., and Kimmins, S. (2015) The histone demethylase KDM1A is essential for the maintenance and differentiation of spermatogonial stem cells and progenitors. *FASEB J.* **29**, 4402–4416
32. Váraljai, R., Islam, A. B., Beshiri, M. L., Rehman, J., Lopez-Bigas, N., and Benevolenskaya, E. V. (2015) Increased mitochondrial function downstream from KDM5A histone demethylase rescues differentiation in pRB-deficient cells. *Genes Dev.* **29**, 1817–1834
33. Wang, C., Wang, J., Li, J., Hu, G., Shan, S., Li, Q., and Zhang, X. (2016) KDM5A controls bone morphogenic protein 2-induced osteogenic differentiation of bone mesenchymal stem cells during osteoporosis. *Cell Death Dis.* **7**, e2335
34. Fattaey, A. R., Helin, K., Dembski, M. S., Dyson, N., Harlow, E., Vuocolo, G. A., Hanobik, M. G., Haskell, K. M., Oliff, A., and Defeo-Jones, D., et al. (1993) Characterization of the retinoblastoma binding proteins RBP1 and RBP2. *Oncogene* **8**, 3149–3156
35. Kim, Y. W., Otterson, G. A., Kratzke, R. A., Coxon, A. B., and Kaye, F. J. (1994) Differential specificity for binding of retinoblastoma binding protein 2 to RB, p107, and TATA-binding protein. *Mol. Cell. Biol.* **14**, 7256–7264
36. Mao, S., Neale, G. A., and Goorha, R. M. (1997) T-cell oncogene rhombotin-2 interacts with retinoblastoma-binding protein 2. *Oncogene* **14**, 1531–1539
37. Konicek, B. W., Stephens, J. R., McNulty, A. M., Robichaud, N., Peery, R. B., Dumstorf, C. A., Dowless, M. S., Iversen, P. W., Parsons, S., Ellis, K. E., McCann, D. J., Pelletier, J., Furic, L., Yingling, J. M., Stancato, L. F., Sonenberg, N., and Graff, J. R. (2011) Therapeutic inhibition of MAP kinase interacting kinase blocks eukaryotic initiation factor 4E phosphorylation and suppresses outgrowth of experimental lung metastases. *Cancer Res.* **71**, 1849–1857
38. Cargnello, M., and Roux, P. P. (2011) Activation and function of the MAPKs and their substrates, the MAPK-activated protein kinases. *Microbiol. Mol. Biol. Rev.* **75**, 50–83
39. Jackson, R. J., Hellen, C. U., and Pestova, T. V. (2010) The mechanism of eukaryotic translation initiation and principles of its regulation. *Nat. Rev. Mol. Cell Biol.* **11**, 113–127
40. Koromilas, A. E., Lazaris-Karatzas, A., and Sonenberg, N. (1992) mRNAs containing extensive secondary structure in their 5′ noncoding region translate efficiently in cells overexpressing initiation factor eIF-4E. *EMBO J.* **11**, 4153–4158
41. Takei, N., Kawamura, M., Hara, K., Yonezawa, K., and Nawa, H. (2001) Brain-derived neurotrophic factor enhances neuronal translation by activating multiple initiation processes: comparison with the effects of insulin. *J. Biol. Chem.* **276**, 42818–42825
42. Furic, L., Rong, L., Larsson, O., Koumakpayi, I. H., Yoshida, K., Brueschke, A., Petroulakis, E., Robichaud, N., Pollak, M., Gaboury, L. A., Pandolfi, P. P., Saad, F., and Sonenberg, N. (2010) eIF4E phosphorylation promotes tumorigenesis and is associated with prostate cancer progression. *Proc. Natl. Acad. Sci. USA* **107**, 14134–14139
43. Genheden, M., Kenney, J. W., Johnston, H. E., Manousopoulou, A., Garbis, S. D., and Proud, C. G. (2015) BDNF stimulation of protein

synthesis in cortical neurons requires the MAP kinase-interacting kinase MNK1. *J. Neurosci.* **35**, 972–984
44. Marcotrigiano, J., Gingras, A. C., Sonenberg, N., and Burley, S. K. (1997) X-ray studies of the messenger RNA 5′ cap-binding protein (eIF4E) bound to 7-methyl-GDP. *Nucleic Acids Symp. Ser.* 36, 8–11
45. Scheper, G. C., and Proud, C. G. (2002) Does phosphorylation of the cap-binding protein eIF4E play a role in translation initiation? *Eur. J. Biochem.* **269**, 5350–5359
46. Vogel, C., Abreu, R. S., Ko, D., Le, S. Y., Shapiro, B. A., Burns, S. C., Sandhu, D., Boutz, D. R., Marcotte, E. M., and Penalva, L. O. (2010) Sequence signatures and mRNA concentration can explain two-thirds of protein abundance variation in a human cell line. *Mol. Syst. Biol.* **6**, 400
47. Araujo, P. R., Yoon, K., Ko, D., Smith, A. D., Qiao, M., Suresh, U., Burns, S. C., and Penalva, L. O. (2012) Before it gets started: regulating translation at the 5′ UTR. *Comp. Funct. Genomics* **2012**, 475731
48. Graff, J. R., Konicek, B. W., Carter, J. H., and Marcusson, E. G. (2008) Targeting the eukaryotic translation initiation factor 4E for cancer therapy. *Cancer Res.* **68**, 631–634
49. Saito, H., Hayday, A. C., Wiman, K., Hayward, W. S., and Tonegawa, S. (1983) Activation of the c-myc gene by translocation: a model for translational control. *Proc. Natl. Acad. Sci. USA* **80**, 7476–7480
50. Rosenwald, I. B., Kaspar, R., Rousseau, D., Gehrke, L., Leboulch, P., Chen, J. J., Schmidt, E. V., Sonenberg, N., and London, I. M. (1995) Eukaryotic translation initiation factor 4E regulates expression of cyclin D1 at transcriptional and post-transcriptional levels. *J. Biol. Chem.* **270**, 21176–21180
51. Graff, J. R., De Benedetti, A., Olson, J. W., Tamez, P., Casero, R. A., Jr., and Zimmer, S. G. (1997) Translation of ODC mRNA and polyamine transport are suppressed in ras-transformed CREF cells by depleting translation initiation factor 4E. *Biochem. Biophys. Res. Commun.* **240**, 15–20
52. Shantz, L. M., and Pegg, A. E. (1994) Overproduction of ornithine decarboxylase caused by relief of translational repression is associated with neoplastic transformation. *Cancer Res.* **54**, 2313–2316
53. Scott, P. A., Smith, K., Poulsom, R., De Benedetti, A., Bicknell, R., and Harris, A. L. (1998) Differential expression of vascular endothelial growth factor mRNA vs protein isoform expression in human breast cancer and relationship to eIF-4E. *Br. J. Cancer* **77**, 2120–2128
54. Yoffe, Y., David, M., Kalaora, R., Povodovski, L., Friedlander, G., Feldmesser, E., Ainbinder, E., Saada, A., Bialik, S., and Kimchi, A. (2016) Cap-independent translation by DAP5 controls cell fate decisions in human embryonic stem cells. *Genes Dev.* **30**, 1991–2004
55. Gkogkas, C. G., Khoutorsky, A., Cao, R., Jafarnejad, S. M., Prager-Khoutorsky, M., Giannakas, N., Kaminari, A., Fragkouli, A., Nader, K., Price, T. J., Konicek, B. W., Graff, J. R., Tzinia, A. K., Lacaille, J. C., and Sonenberg, N. (2014) Pharmacogenetic inhibition of eIF4E-dependent Mmp9 mRNA translation reverses fragile X syndrome-like phenotypes. *Cell Reports* **9**, 1742–1755

Received for publication August 7, 2017.
Accepted for publication November 27, 2017.